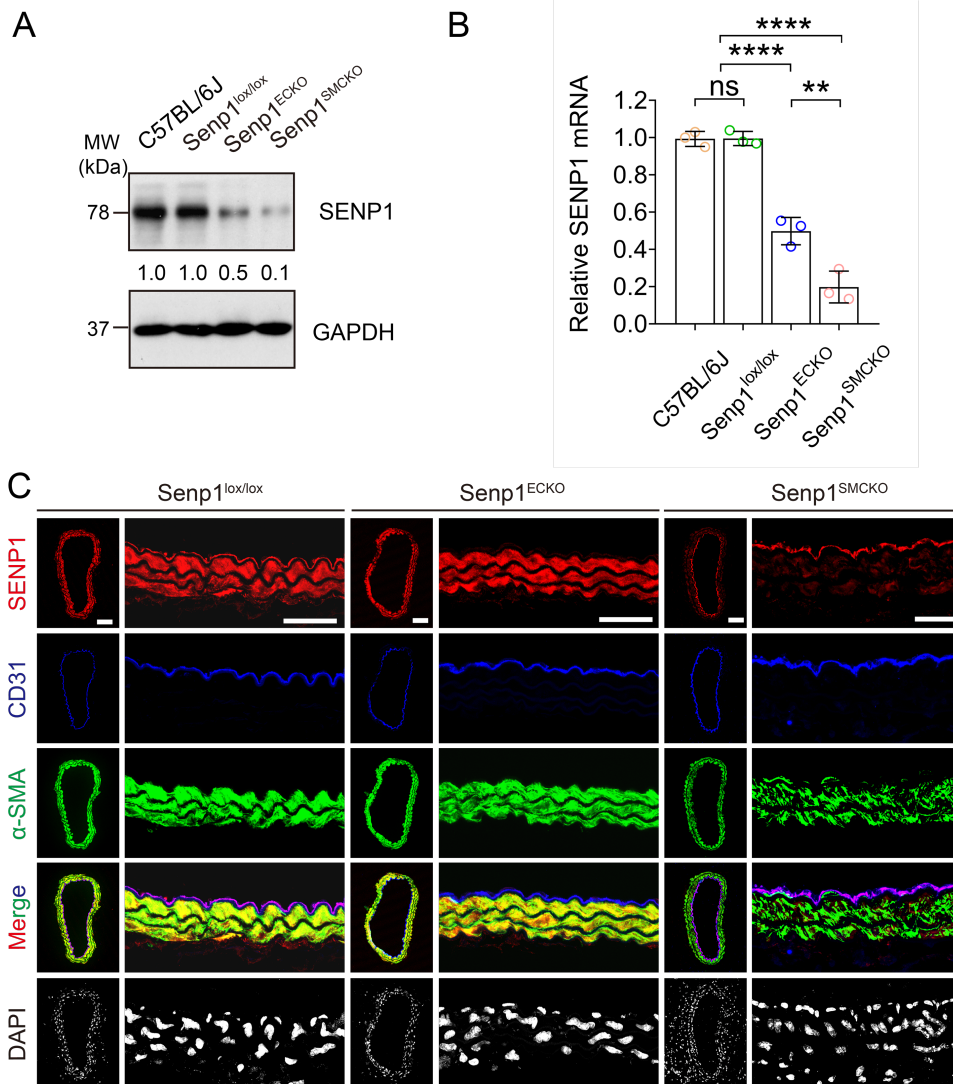


SUPPLEMENTAL MATERIALS

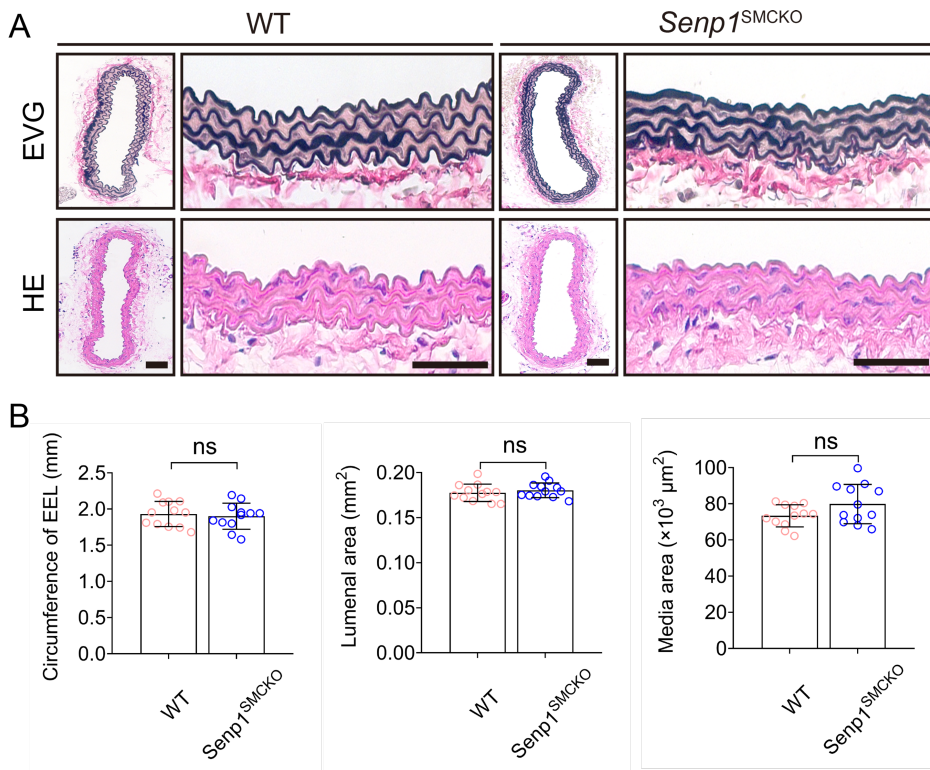
SRF SUMOylation modulates smooth muscle phenotypic switch and vascular remodeling

Yue Xu, Haifeng Zhang, Jordan S. Pober, Wang Min, and Jenny Huanjiao Zhou

SUPPLEMENTAL DATA



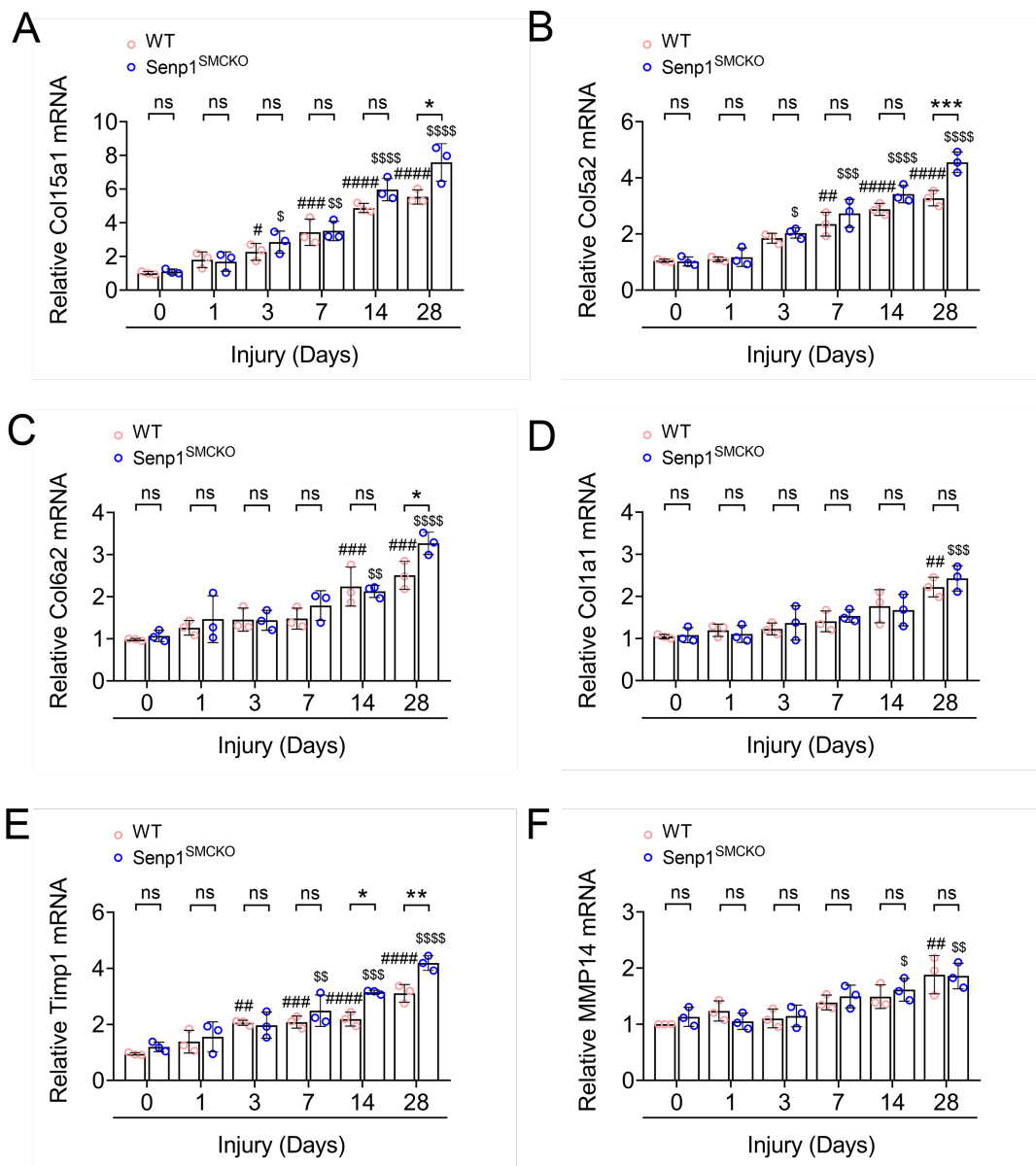
Supplemental Fig. 1. Generation of VSMCs or ECs-specific Senp1 gene knockout mice. A. The protein levels of Senp1 in the normal carotid arteries from C57BL/6, *Senp1*^{lox/lox}, *Senp1*^{ECKO} and *Senp1*^{SMCKO} mice at age of 10-12 weeks (all in C57BL/6 background) were determined by western blot. GAPDH was served as a control. Relative protein levels are presented by taking C57BL/6 as 1.0 (n=3). **B.** The mRNA levels of Senp1 in the normal carotid arteries from C57BL/6, *Senp1*^{lox/lox}, *Senp1*^{ECKO} and *Senp1*^{SMCKO} mice were determined by RT-PCR. GAPDH was served as a control. Relative mRNA levels are presented by taking C57BL/6 as 1.0 (n=3). Data are mean \pm SEM. **** P < 0.0001. One-way ANOVA with Bonferroni post hoc analysis. **C.** Immunofluorescence triple staining of normal carotid arteries with specific antibodies against Senp1 (red), α -SMA (green) and CD31 (APC-conjugated and pseudo-colored by blue). Nuclei were stained with DAPI (pseudo-colored by white). Yellow indicates the co-localization of Senp1 with α -SMA, and purple indicates the co-localization of Senp1 with CD31 in the merged images. Scale bars, 50 μ m.



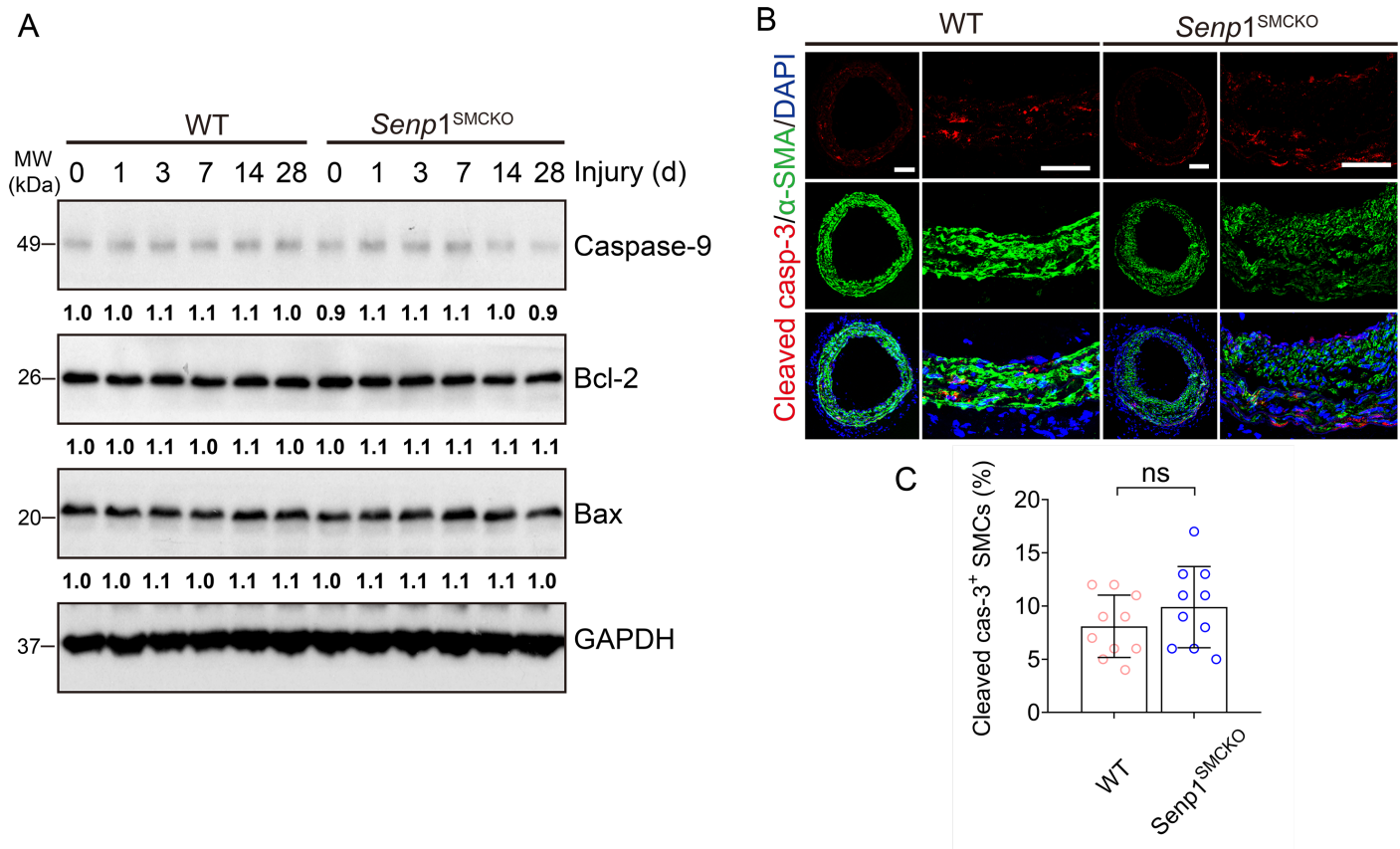
C Gene expression altered in *Senp1*^{SMCKO} vs WT

	WT	Senp1 ^{SMCKO}		
Proliferation	Ccnd1	-0.0305	-0.0412	-0.0346
	Pcna	0.449	0.498	0.454 *
	Cdk2	-0.713	-0.823	-0.634 *
	Cdkn1b	-0.314	-0.434	-0.332 *
	Ccne1	0.18	0.212	0.154 *
	Cdh13	0.0983	0.0839	0.0715
Contractile	Acta2	-0.871	-0.76	-0.96 *
	Myh11	-0.428	-0.308	-0.48 *
	Ccn1	0	0.002	0.0004
	Tagln	0.018	-0.1670715	0.0021
	Myl6	0.328	0.386	0.493 *
	Myl9	-1.136	-1.351	0.133
Synthetic	Opn	-0.24	-0.403	0.024
	Myl10	0	0.003	-0.0004
	Col5a1	-0.00049	-0.00021	0.00019
	Col6a2	0.0789	-0.00025	0.0446
	Col18a1	0.166	0.305	0.102 *
	Mmp2	-0.674	-0.451	-0.172 *
	Mmp9	1.075	0.911	0.874 *
	Mmp14	-0.476	-0.677	-0.729 *
	Mfap5	0.5218	0.3617	0.636 *
Inflammation	Vcan	0.401	0.512	0.08
	Vcam1	0.316	0.34	0.67 *
	Cxcl1	0.05	0.0336	0.036
	Cd68	0.0441	0.0419	0.0481
	Il33	0.816	0.632	0.485 *
	Il4ra	0.415	0.392	0.317 *
	Il6ra	0.4528	0.495	0.311 *
	Ccl3	-0.141	0.00024	0

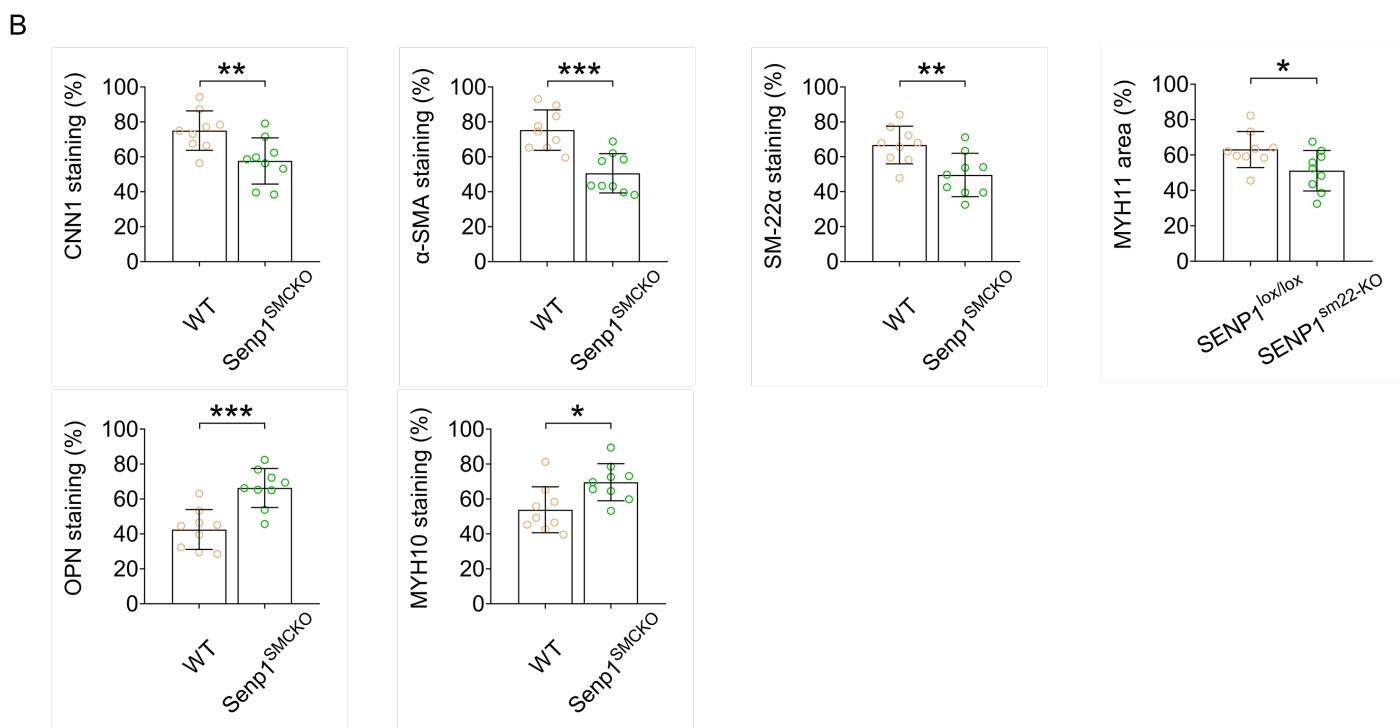
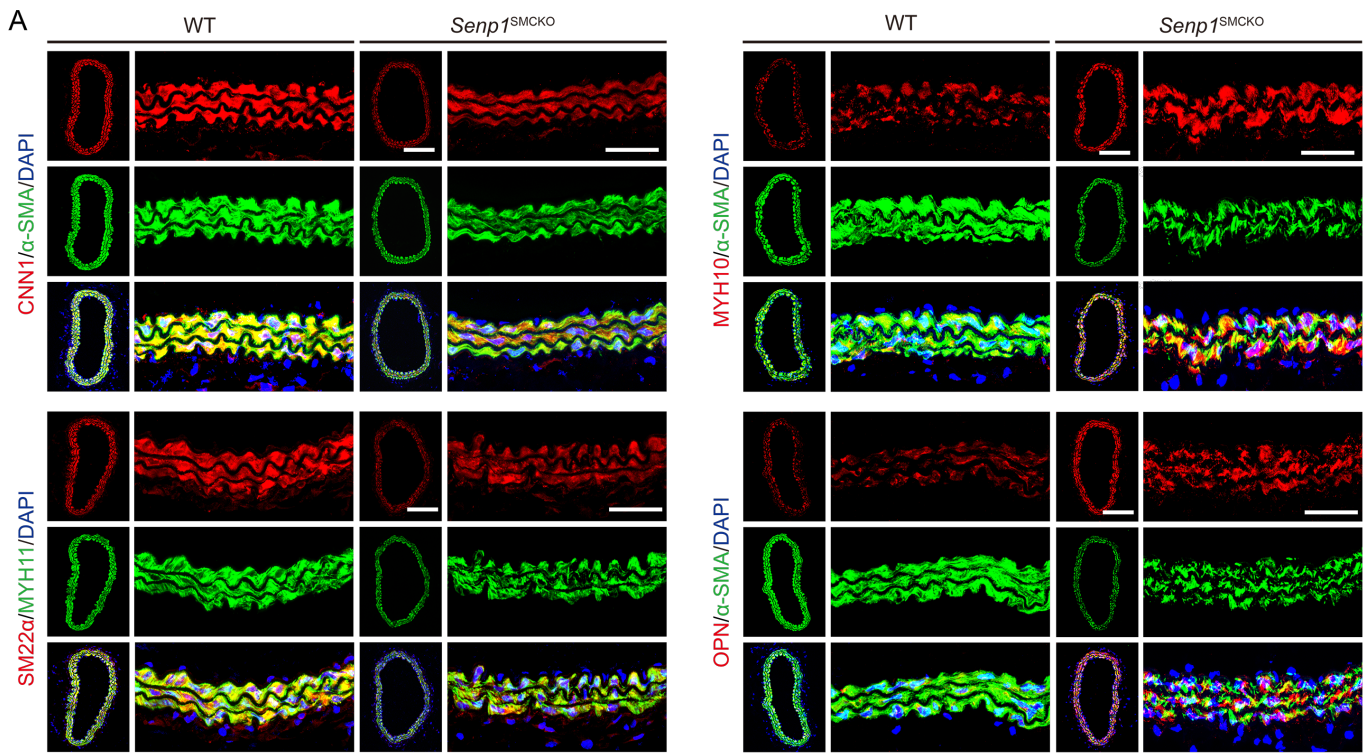
Supplemental Fig. 2. The histological and morphometric features of carotid arteries between *Senp1*^{lox/lox} (WT) and *Senp1*^{SMCKO} mice in baseline conditions. A. Representative photomicrographs of EVG staining and HE staining. **B.** The circumference of EEL, luminal area and media area in normal carotid arteries from WT and *Senp1*^{SMCKO} mice at 10-12 weeks of age (n=12 per group). Data are mean \pm SEM. ns, no significance, using two-tailed Student's t-test. EVG: elastic van gieson; HE: haematoxylin and eosin; EEL indicates external elastic lamina. Scale bars: 50 μ m. **C.** Total RNAs were isolated from carotid arteries without injury and were subjected to RNA-sequencing analyses (n=3 per group). Heat map showing the gene expression of proliferation, contractile phenotype, synthetic phenotype, and inflammation in carotid arteries of WT and *Senp1*^{SMCKO} mice. Asterisks indicate statistical significances ($p<0.05$) using two-tailed Student's t-test.



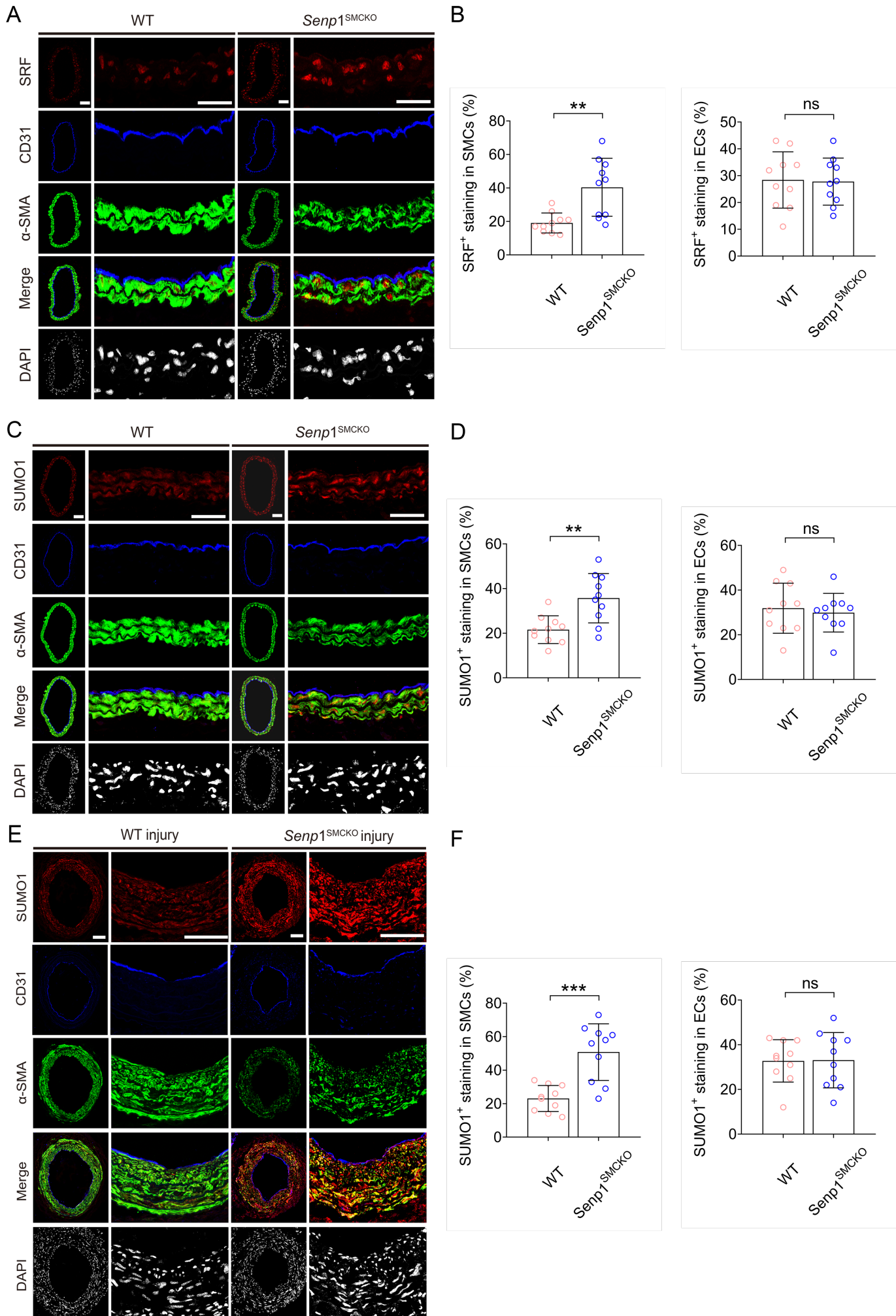
Supplemental Fig. 3. *Senp1* deficiency in VSMCs increases multiple ECM-related genes expression during vascular remodeling. *Senp1*^{lox/lox} (WT) and *Senp1*^{SMCKO} mice at age of 10-12 weeks were subjected to wire injury on left carotid arteries, and carotid arteries were harvested for analyses on day 3-28 post-injury as indicated. Non-injured mice were used as controls (time 0). Total RNAs were used for RT-PCR for mRNA levels of ECM-related genes. Gapdh as a control. Col15a1 (A), Col5a2 (B), Col6a2 (C), and Col1a1 (D), Tim1 (E) and Mmp14 (F). Data are mean \pm SEM. * P < 0.05; ** P < 0.01; *** P < 0.001; **** P < 0.0001; ns, no significance, Two-tailed Student's t-test. # P < 0.05; ## P < 0.01; ### P < 0.001; ##### P < 0.0001, compared with un-injury WT mice; \$ P < 0.05; \$\$ P < 0.01; \$\$\$ P < 0.001; \$\$\$\$ P < 0.0001, compared with un-injury *Senp1*^{SMCKO} mice, using one-way ANOVA with Bonferroni post hoc analysis.



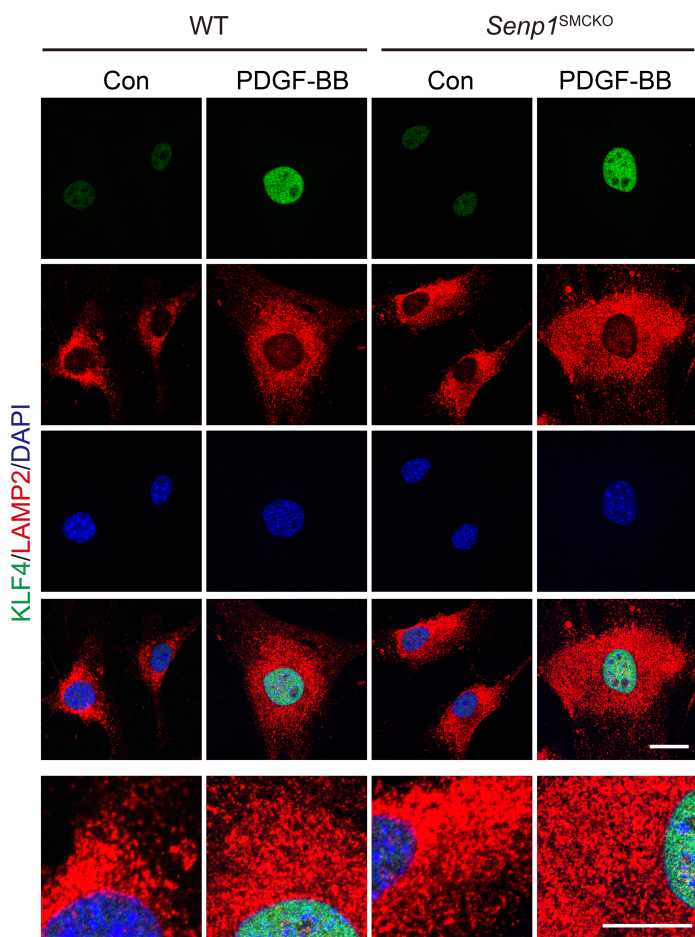
Supplemental Fig. 4. *Senp1* deficiency in VSMCs does not affect apoptosis in neointima. *Senp1*^{lox/lox} (WT) and *Senp1*^{SMCKO} mice at age of 10-12 weeks were subjected to wire injury on left carotid arteries, and carotid arteries were harvested for analyses on day 3-28 post-injury as indicated. Non-injured mice were used as controls (time 0). **A.** Western blots showing the protein levels of caspase-9, Bcl-2 and Bax in carotid arteries of WT and *Senp1*^{SMCKO} mice (n=3 per group). GAPDH served as the control. Relative protein levels are presented by taking WT as 1.0 (n=3). **B.** Immunofluorescence double staining showing the expression and co-localization of cleaved caspase-3 (red) and α-SMA (green) in neointima of WT and *Senp1*^{SMCKO} mice at 28 days after wire injury. Nuclei were stained with DAPI (blue). Scale bars: 50 μm. **C.** Quantitative analysis of the percentages of cleaved caspase-3-positive stained VSMCs. Data are mean ± SEM (n=10 per group). ns, no significance, using two-tailed Student's t-test.



Supplemental Fig. 5. *Senp1* deficiency in VSMCs weakly down-regulated basal levels of VSMC contractile markers. A. Carotid arteries on day 0 were subjected to immunofluorescence co-staining of various contractile and synthetic markers as indicated with DAPI counterstaining for nuclei (blue). **B.** MFI of each marker within the media layer was quantified (n=10 per group). Data are mean \pm SEM. * P < 0.05; ** P < 0.01; *** P < 0.001; **** P < 0.0001; ns, no significance. Two-tailed Student's t-test. MFI: mean fluorescence intensity.



Supplemental Fig. 6. The expressions of SRF and SUMO1 in carotid arteries between *Senp1*^{lox/lox} (WT) and *Senp1*^{SMCKO} mice. A-B. Immunofluorescence staining for SRF in carotid arteries from WT and *Senp1*^{SMCKO} mice on day 0. **(A)** Four color images are presented with SRF (red), α -SMA (green), CD31 (APC; pseudo-colored by blue) and DAPI (blue; pseud-colored by white). **(B)** MFI of SRF within the media layer or ECs was quantified (n=10 per group). **C-D.** Immunofluorescence staining for SUMO1 in carotid arteries from WT and *Senp1*^{SMCKO} mice on day 0. **(C)** Four color images are presented with SUMO1 (red), α -SMA (green), CD31 (APC; pseudo-colored by blue) and DAPI (blue; pseud-colored by white). **(D)** MFI of SUMO1 within the media layer or ECs was quantified (n=10 per group). **E-F.** Immunofluorescence staining for SUMO1 in carotid arteries from WT and *Senp1*^{SMCKO} mice on day 28 post-injury. **(E)** Four color images are presented with SUMO1 (red), α -SMA (green), CD31 (APC; pseudo-colored by blue) and DAPI (blue; pseud-colored by white). **(F)** MFI of SUMO1 within the neointimal areas and ECs were quantified (n =10 per group). Data are mean \pm SEM. ** P < 0.01. Two-tailed Student's t-test. Scale bars, 50 μ m (left) and 20 μ m (right). MFI: mean fluorescence intensity.



Supplemental Fig. 7. SENP1 deletion has no effect on KLF4 cellular localization. A-B. VSMCs Isolated from un-injured WT and *Senp1*^{SMCKO} mice were treated with PDGF-BB for 24 h. Cells were subjected to immunofluorescence co-staining with KLF4 and LAMP2. High magnification of merged images is shown at the bottom of each panel. Lysosomal and nuclear KLF4 are indicated by arrows and arrowheads, respectively.

 Motifs with high probability
 Motifs with low probability

Homo sapiens	129	GA VSGAKPGKKT RGRVK IKMEF IDNKLRRYTT FSK RKTG IMK KAY 173
Mus musculus	125	GA VSGAKPGKKT RGRVK IKMEF IDNKLRRYTT FSK RKTG IMK KAY 169
Rattus norvegicus	125	GA VSGAKPGKKT RGRVK IKMEF IDNKLRRYTT FSK RKTG IMK KAY 169
Canis lupus familiaris	129	GA VSGAKPGKKT RGRVK IKMEF IDNKLRRYTT FSK RKTG IMK KAY 173
Gallus gallus	69	GE RRGL KRGL AE AA.....GAVSG AKPG KKTRGR VK IKME FIDN KLR 140
	143TT FSK RKTG IMK KAYELS.....SGSSLTELQV VNLDTSHN AK SD 492

Homo sapiens			
NO.	Pos.	Group	Score
1	K147	RGRVK IKME FIDNK	0.94
2	K135	GAVSG AKPG KKT	0.62
3	K165	TTFSK RKTG IMKKA	0.27

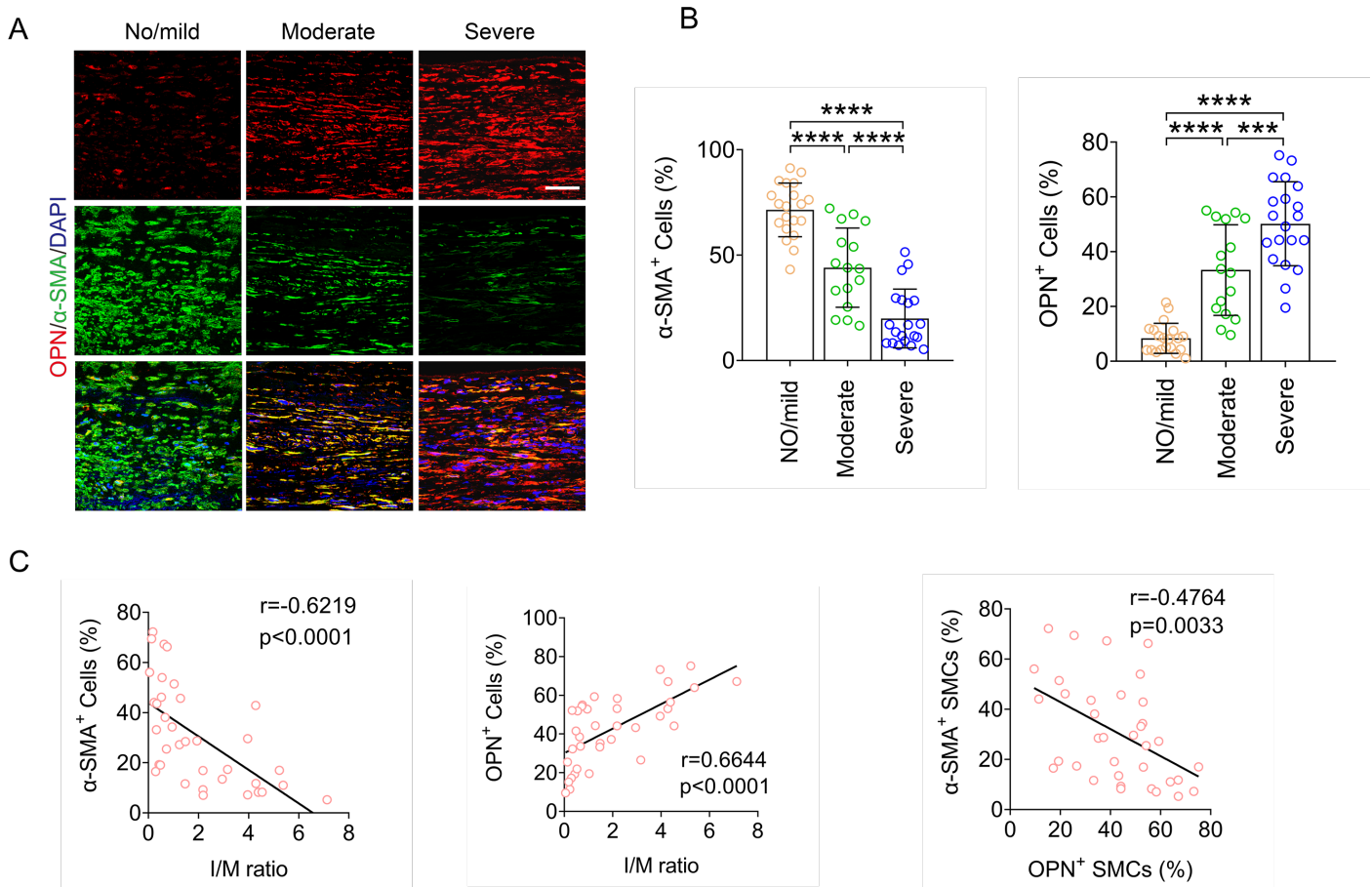
Canis lupus familiaris			
NO.	Pos.	Group	Score
1	K147	RGRVK IKME FIDNK	0.94
2	K135	GAVSG AKPG KKT	0.62
3	K165	TTFSK RKTG IMKKA	0.27

Mus musculus			
NO.	Pos.	Group	Score
1	K143	RGRVK IKME FIDNK	0.94
2	K131	GAVSG AKPG KKTRG	0.62
3	K161	TTFSK RKTG IMKKA	0.27

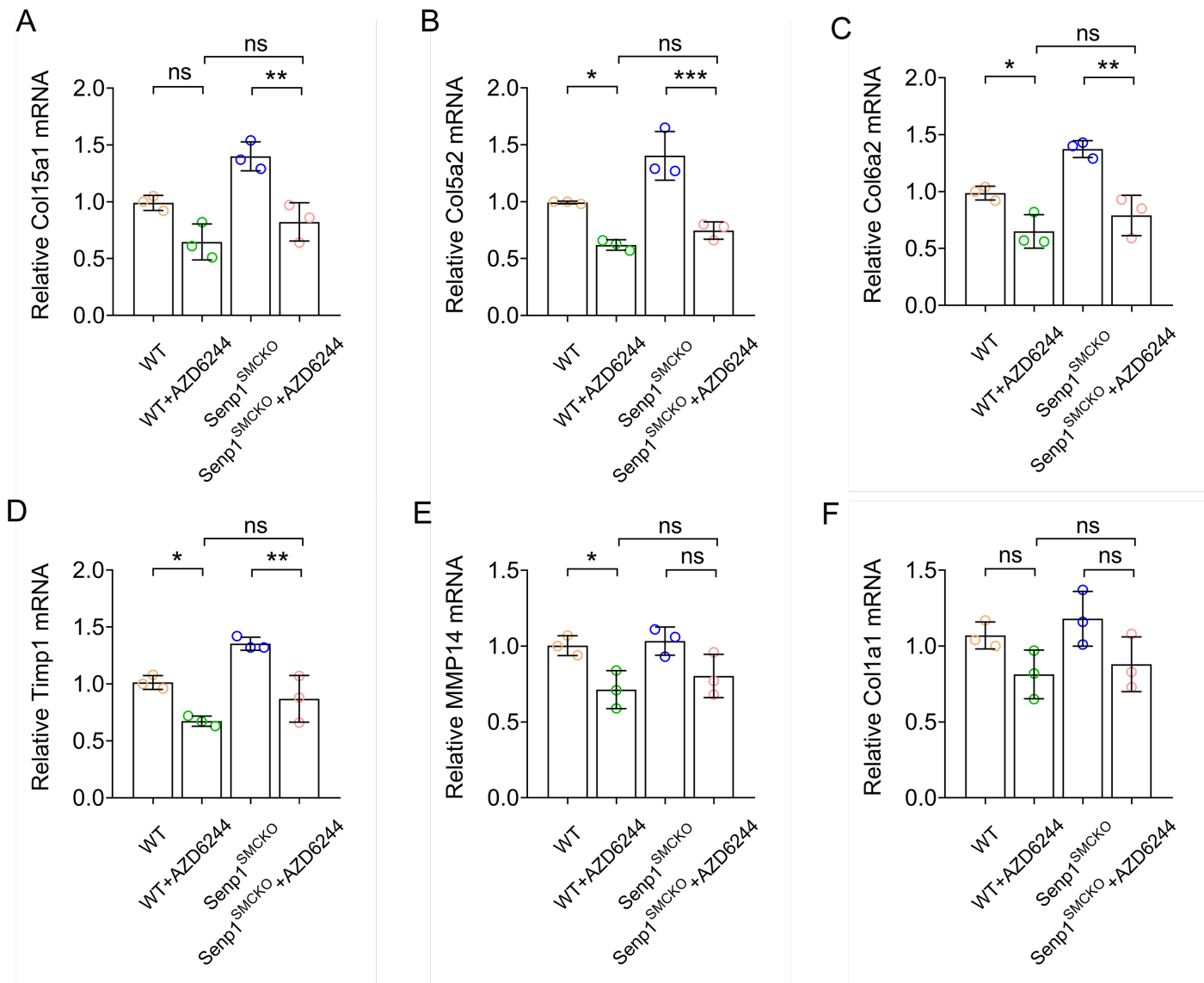
Gallus gallus			
NO.	Pos.	Group	Score
1	K131	RGRVK IKME FIDNK	0.94
2	K490	DTSHN AKSD	0.79
3	K75	GERRG LKRG LAEAA	0.73
2	K119	GAVSG AKPG KKTRG	0.62
3	K149	TTFSK RKTG IMKKA	0.27

Rattus norvegicus			
NO.	Pos.	Group	Score
1	K143	RGRVK IKME FIDNK	0.94
2	K131	GAVSG AKPG KKTRG	0.62
3	K161	TTFSK RKTG IMKKA	0.27

Supplemental Figure 8. Conservation of vertebrate SRF proteins at the SUMOylation sites. SRF protein sequence comparison among Homo sapiens, Mus musculus, Rattus norvegicus, Canis lupus familiaris, and Gallus gallus. The potential SUMO motifs are marked in red and blue, indicating their high and moderate conservations among species, respectively.



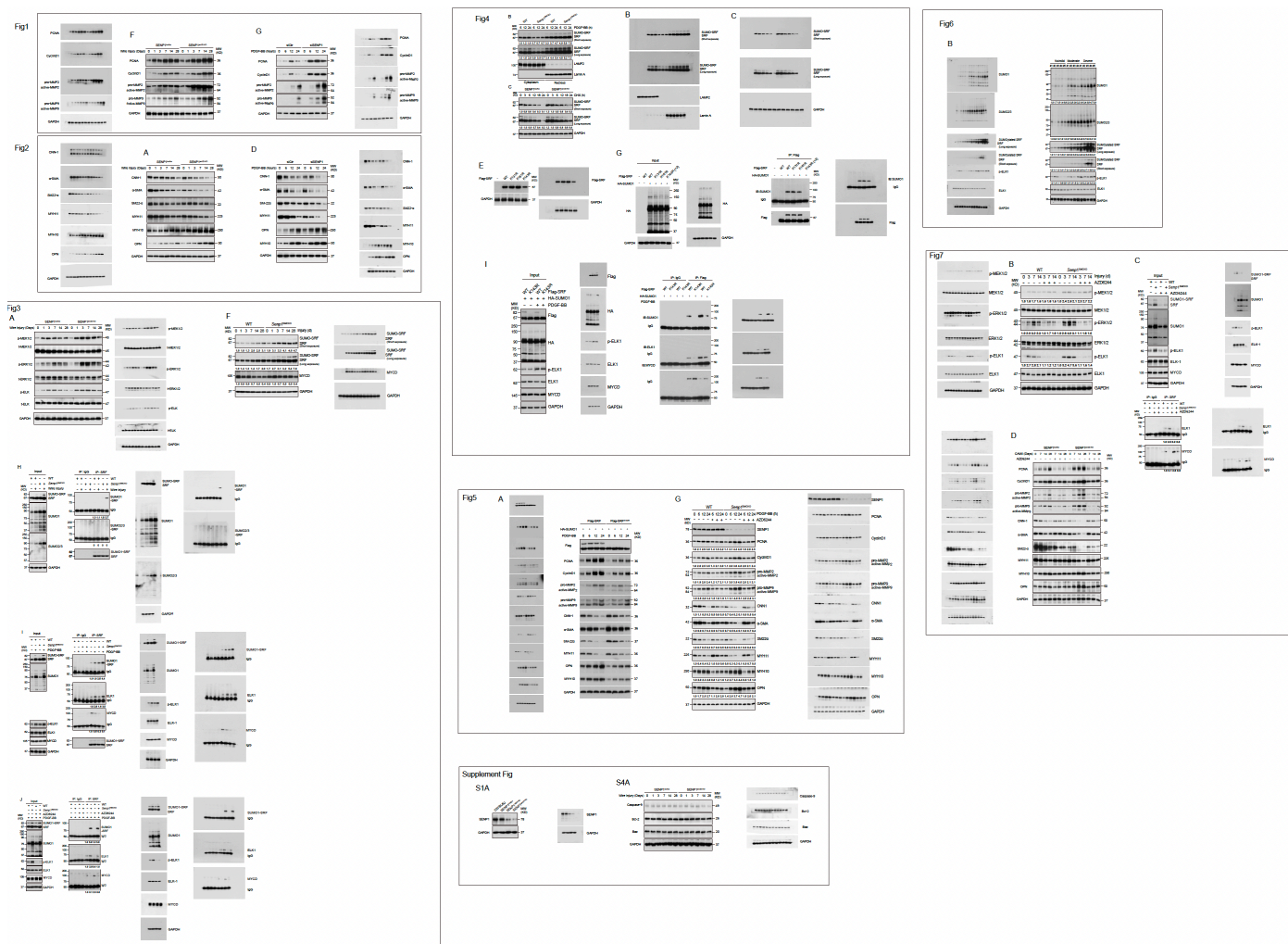
Supplemental Figure 9. Correlations of α-SMA and OPN in VSMCs with neointimal formation in human specimens. **A.** Immunocytochemical analysis of OPN and α-SMA expressions in the VSMCs of left main coronary arteries of patients with no/mild ($n = 5$), moderate ($n = 4$), and severe ($n = 5$) CAD. Five fields per section from each sample are analyzed. Representative images of immunofluorescence staining for α-SMA (green) and OPN (red). Nuclei were stained with DAPI (blue). Scale bar: 20 μ m. Yellow indicates the colocalization of OPN with α-SMA and DAPI in the merged images. **B.** Quantitative analysis of α-SMA or OPN-positive cells in the lumen. Data are mean \pm SEM. *** $P < 0.001$; **** $P < 0.0001$ (One-way ANOVA with Bonferroni post hoc analysis). **(C)** Scatter plots of I/M ratio, OPN and α-SMA. The corresponding Spearman's correlation coefficient (r) between I/M ratio, OPN and α-SMA, and the P value are shown. Data are mean \pm SEM. * $P < 0.05$; ** $P < 0.01$; *** $P < 0.001$; **** $P < 0.0001$, ns, no significance. Correlation analyses between variables were performed using the Pearson rank correlation test. P values were two-tailed and values <0.05 was considered statistically significant.



Supplemental Fig. 10. The effect of AZD6244 on gene expression of ECM during vascular remodeling.

A-F. Real-time PCR showing the mRNA levels of Col15a1 (**A**), Col5a2 (**B**), Col6a2 (**C**), Timp1 (**D**) and MMP14 (**E**) and Col1a1 (**F**) in carotid arteries of WT and *Senp1^{SMCKO}* mice at 28 days after wire injury with or without AZD6244 treatment (n=3 per group). Gapdh served as the control. Data are mean \pm SEM. * P < 0.05; ** P < 0.01; *** P < 0.001; ns, no significance. One-way ANOVA with Bonferroni post hoc analysis.

Supplemental Fig.11: Uncut original gels



Supplemental Table 1: Demographic details of the human coronary arteries samples.

Subject	Diagnosis	Ages (years)	Gender
1	trauma	44	Male
2	trauma	63	Male
3	trauma	51	Male
4	trauma	38	Female
5	trauma	55	Male
6	coronary heart disease	71	Male
7	coronary heart disease	67	Male
8	coronary heart disease	66	Female
9	coronary heart disease	58	Male
10	coronary heart disease	64	Male
11	coronary heart disease	56	Female
12	coronary heart disease	74	Male
12	coronary heart disease	68	Male
14	coronary heart disease	76	Male

Supplemental Table 2. List of RT-qPCR primers and sequences.

Name	Forward	Reserve
m- α -SMA	5'-TGACCCAGATTATGTTGAGACCT-3'	5'-TCCAGAGTCCAGCACAATACCA-3'
m-SM22 α	5'-GTTCCAGACTGTTGACCTCTTG-3'	5'-TGTCTGTGAACCTCCCTTATGCT-3'
m-CNN-1	5'-ACGACCACCAGCGTGAGCA-3'	5'-CTGGGTTGACTCATTGACTCATTGACCTTCTT-3'
m-MYH11	5'-TGAGCTCAGTGACAAGGTCCACAA-3'	5'-GGAAGCCACATCTTGGCCAGTTT-3'
m-MYH10	5'-CGACCGGTGCCAACGCATC-3'	5'-GACACAGTTGATCTTCAGGAAGG-3'
m-OPN	5'-GATGATGATGACGATGGAGACC-3'	5'-CGACTGTAGGGACGATTGGAG-3'
m-SENP1	5'-CTGGGGAGGTGACCTTAGTGA-3'	5'-GTGATAATCTGGACGATAGGCTG-3'
m-Col5a2	5'-GTGTCTGTGACAATGGTGCC-3'	5'-AGAGCCAGGCATGAGTCCTA-3'
m-Col6a2	5'-GAGCGAGTCAACTCCCTGTC-3'	5'-CCATCCAGCAGGAAGACAAT-3'
m-Col15a1	5'-CTGTCCACTTCCGAGCCTT-3'	5'-AAAGCACTTGGCCCTTGAGA-3'
m-Colla1	5'-GGCTGCACGAGTCACAC-3'	5'-TGGAGGGAGTTACACGAAG-3'
m-Timp1	5'-ACTCGGACCTGGTCATAAGGGC-3'	5'-TTCCGTGGCAGGCAAGCAAAGT-3'
m-Mmp14	5'-CAAGGCCAATGTTGGAGGAAG-3'	5'-TCTCCCATACTCGGAAGGCCTTC-3'
m- β -actin	5'-GGCTGTATTCCCCTCCATCG-3'	5'-CCAGTTGGTAACAATGCCATGT-3'
m-GAPDH	5'-CATGAGAAGTATGACAACAGCCT-3'	5'-AGTCCTTCCACGATACCAAAGT-3'
m-SRF	5'-CCAGCGCTGTCAGCAGTGCAAC-3'	5'-GCTGCTCCCAGCTTGTGCCCTATC-3'
m-SRF-K143R	5'-CGCGTGAAGATCAGGATGGAGTTCATC-3'	5'-GATGAACTCCATCCTGATCTCACGCG-3'
m-SRF-K131R	5'-GTGAGCGGGGCCAGGCCGGGAAGAAG-3'	5'-CTTCTTCCCCGGCCTGGCCCCGCTCAC-3'
m-SRF-K135R	5'-GTGAGCGGGGCCAGGCCGGTAAGAAG-3'	5'-CTTCTTACCCGGCCTGGCCCCGCTCAC-3'
m-SRF-K161R	5'-TTCAGCAAGAGGAGGGACGGGCATCATG-3'	5'-CATGATGCCGTCCCTCTTGCTGAA-3'

Supplemental Table 3: Antibodies used in this study.

Name	CAS	Source	Dilution/IF	Dilution/WB
α -SMA	Sigma F3777-2ML	M	1:300/mouse 1:100/human	
α -SMA	Invitrogen 14-9760-82	M		1:500/mouse
SM-22 α	Abcam ab10135	G	1:50/mouse	1:500/mouse
MYH11	Abcam ab53219	Rb	1:200/mouse	1:1000/mouse
Calponin1 (CNN1)	Abcam ab46794	Rb	1:200/mouse	1:500/mouse
Osteopontin (OPN)	Abcam ab8448	Rb	1:200/human	
Osteopontin (OPN)	Abcam ab218237	M	1:1000/mouse	1:1000/mouse
MYH10	Abcam ab230823	Rb	1:200/mouse	1:500/mouse
MMP2	Abcam ab37150	Rb	1:200/mouse	1:500/mouse
MMP9	Abcam ab38898	Rb	1:200/mouse	1:500/mouse
SENP1	Cell signaling CST11929s	Rb		1:1000/human
SENP1	Abcam ab236094	Rb	1:200/mouse	
SENP1	Life science D2614000200	Rb		1:500/human
SENP1	Invitrogen ZYMED383350	Rb	1:200/human	1:500/mouse
SENP1	Santa cruz sc271360	M		1:500/mouse
SUMO1	Cell signaling CST4930s	Rb	1:200/mouse 1:100/human	
SUMO1	Santa cruz sc5308	M		1:1000/mouse 1:500/human
SUMO2/3	Santa cruz sc393144	M	1:200/mouse 1:100/human	
SRF	Cell signaling CST5147s	Rb	1:200/mouse 1:100/human	1:1000/mouse 1:500/human 1:50/mouse (Co-IP)
CyclinD1	Cell signaling CST2978	Rb		1:1000/mouse
PCNA	Cell signaling CST13110	Rb		1:500/mouse
Ki67	Abcam ab66155	Rb	1:300/mouse	

CD31	Millipore MAB13982	H	1:500/mouse	
CD31	R&D Systems AF3628	G	1:500/mouse	
Myocardin	Sigma-Aldrich SAB4200539	Rb		1:500/mouse
p-MEK1/2	Cell signaling CST2338	Rb		1:1000/mouse
MEK1/2	Cell signaling CST8727	Rb		1:1000/mouse
p-ELK1	Santa cruz sc8406	M	1:50/mouse	1:200/mouse
ELK1 (E-5)	Santa cruz sc365876	M		1:500/mouse
p-ERK1/2	Cell signaling CST4370s	Rb		1:1000/mouse
ERK1/2	Santa cruz sc514302	M		1:2000/mouse
p-NF-κB	Cell signaling CST3033s	Rb		1:1000/mouse
NF-κB	Cell signaling CST8242s	Rb		1:1000/mouse
p-P38	Cell signaling CST4511s	Rb		1:1000/mouse
P38	Cell signaling CST8690	Rb		1:1000/mouse
HA-Tag	Cell signaling CST3724	Rb	1:300/mouse	1:1000/mouse
DYKDDDDK Tag (Flag)	Cell signaling CST14793	Rb	1:300/mouse	1:2000/mouse
Cleaved caspase-3	Cell signaling CST9579T	Rb		1:200/mouse
Caspase-9	Cell signaling CST9504	Rb		1:500/mouse
Bcl-2	Cell signaling CST15071	M		1:1000/mouse
BAX	Cell signaling CST14796	Rb		1:500/mouse
GAPDH	Cell signaling CST5174s	Rb		1:5000/mouse 1:5000/human
LAMP2	Abcam Ab13524	Rat	1:300	1:1000
KLF4	Abcam Ab151733	Rb	1:500	